Electronic Supplementary Information

Assembly of [$Cu_2(COO)_4$] and [$M_3(\mu_3\text{-}O)(COO)_6$] (M = Sc, Fe, Ga, and In) Building Blocks into Porous Frameworks towards Ultra-High C_2H_2/CO_2 and C_2H_2/CH_4 Separation Performance

Jian-Wei Zhang,[a,b] Man-Cheng Hu,[a] Shu-Ni Li,[a] Yu-Cheng Jiang,[a] Peng Qu[b] and Quan-Guo Zhai*[a]

[a]Key Laboratory of Macromolecular Science of Shaanxi Province, Key Laboratory of Applied Surface and Colloid Chemistry, Ministry of Education, School of Chemistry & Chemical Engineering, Shaanxi Normal University, Xi'an, Shaanxi, 710062, P. R. China.

[b]Henan Key Laboratory of Biomolecular Recognition and Sensing,
School of Chemistry and Chemical Engineering,
Shangqiu Normal University, Shangqiu, 476000, P.R. China.

*E-mail: zhaiqg@snnu.edu.cn (Q. G. Zhai)

S1. Experimental Section in Electronic Supplementary Information

Materials and methods

All chemicals were purchased from commercial sources and used as received without further purification. The powder X-ray diffraction (PXRD) patterns were collected on a Rigaku MiniFlex600 (40 kV, 15 mA) diffractometer Cu Kα (λ = 1.54056 Å) at room temperature. Thermogravimetric analyses (TGA) were carried out on a NETZSCH STA 449C thermal analyzer at a heating rate of 2 °C/min under nitrogen. Scanning Electron Microscope (SEM) images were taken on a Philips-FEI Quanta 200. The semi-quantitative elemental analyses of different samples were performed by using Philips-FEI Quanta 200) equipped with energy dispersive spectroscopy (EDS) detector. The Zeta potential analysis was done by the Malvern Zetasizer. The solid state ^{13}C crosspolarization magicangle spinning (CP/MAS) NMR spectroscopy was performed by Bruker AVANCE III 400 Solid State NMR.

Synthesis of $[M_3Cu_6(O)(H_2O)_8(OH)(PTC)_6]$ (M = Sc, Fe, Ga and In) (SNNU-65s)

Prior to synthesis, 0.2 M aqueous solution of $Cu(NO_3)_2$, $Sc(NO_3)_3$, $Fe(NO_3)_3$, $Ga(NO_3)_3$ and $In(NO_3)_3$ were firstly prepared.

Synthesis of SNNU-65-Cu-Ga

H_3PTC (10 mg, 0.035 mmol) was added to DMF/dioxane (2.4 mL/0.4 mL), after clear, 0.14 mL freshly prepared 0.2 M solution of $Ga(NO_3)_3$ was added, followed by the addition of 0.4 mL 0.2 M solution of $Cu(NO_3)_2$, and then 0.5 mL acetic acid was added. The mixture was sealed in a 20 mL glass vial and ultrasonicated to give a clear solution, and placed in an oven preheated at 85 ^oC for 20 h. After that, it was cooled down to room temperature. The resulting crystals were washed with DMF and CH_2Cl_2 and then dried in air. The yield was about 60% based on H_3PTC.

Synthesis of SNNU-65-Cu-Sc and -Cu-Fe

SNNU-65-Cu-Sc and **SNNU-65-Cu-Fe** were obtained by a procedure similar to that of **SNNU-65-Cu-Ga**, except that $Sc(NO_3)_3$ and $Fe(NO_3)_3$ were used in place of $Ga(NO_3)_3$, respectively. The yield were about 82% and 78% (based on H_3PTC), respectively.

Synthesis of SNNU-65-Cu-In

H_3PTC (30 mg, 0.10 mmol) was added to DMF/dioxane (2.4 mL/0.4 mL), after clear, 0.42 mL freshly prepared 0.2 M aqueous solution of $In(NO_3)_3$ was added, followed by the addition of 1.2 mL 0.2 M solution of $Cu(NO_3)_2$, and then 0.5 mL acetic acid was added. The followed procedure was similar to that of **SNNU-65-Cu-Ga**. The yield was about 75% based on H_3PTC.

Single-Crystal X-ray Crystallograpic Determination

Single crystal X-ray data collection for porous coordination compound was performed on Bruker D8 Photon 100 CMOS diffractometer equipped with a graphite-monochromated Mo Kα radiation (λ = 0.71073 Å). The SADABS program was used for absorption correction. The structures were solved by Patterson method for **SNNU-65-Cu-Ga**. The structure refinements were based on $|F|^2$ with anisotropic displacement using *SHELXTL*.[1] All non-hydrogen atoms in the framework were refined with anisotropic displacement parameters. For about the **SNNU-65-Cu-Ga**, the residual Q peaks probably correspond to highly disordered solvent molecules were treated using the SQUEEZE routine in the PLATON software package.[2] These crystal data can be obtained free of charge from The Cambridge Crystallographic Data Centre through www.ccdc.cam.ac.uk/data_request/cif.

Gas Adsorption

Gas sorption isotherms were measured on a Micromeritics ASAP 2020 HD88 surface-area and pore-size analyzer up to 1 bar of gas pressure by the static volumetric method. All used gases were of 99.99% purity. To probe the effect of key structural parameters on the interactions of frameworks and gas molecules, all as-synthesized samples were activated by immersion in DMF for one day, followed by exchange into acetone three times over the course of four days. The solvent-exchanged crystals were then loaded in sample tubes and activated under high vacuum at 80 °C for 20 h. The gas sorption isotherms for N_2 and H_2 were measured at 77 K with liquid nitrogen. The gas sorption isotherms for Ar were measured at 87 K. The gas sorption isotherms for CO_2, CH_4, C_2H_2, and C_2H_4 were measured at 273 and 298 K, respectively.

Estimation of the isosteric heats of gas adsorption

To extract the coverage-dependent isosteric heat of adsorption for compounds, the data were modeled with a virial-type expression[3] composed of parameters a_i and b_i that are independent of temperature:

$$\ln P = \ln N + \frac{1}{T}\sum_{i=0}^{m} a_i N^i + \sum_{i=0}^{n} b_i N^i \qquad (1)$$

$$Q_{st} = - R\sum_{i=0}^{m} a_i N^i \qquad (2)$$

Where P is pressure, N is the amount adsorbed (or uptake), T is temperature, and m and n determine the number of terms required to adequately describe the isotherm. R is the universal gas constant. The coverage dependencies of Q_{st} calculated from fitting the data at 273 K and 298 K under the pressure range from 0-1 bar, and Q_{st} and R is the universal gas constant.

Selectivity Prediction for Binary Mixture Adsorption

Ideal adsorbed solution theory (IAST)[4] was used to predict binary mixture adsorption from the experimental pure-gas isotherms. To perform the integrations required by IAST, the single-component isotherms should be fitted by a proper model.

The Langmuir–Freundlich (LF) equation was found to the best fit to the experimental pure isotherms for CO_2, C_2H_2, and C_2H_4 and CH_4 of **SNNU-65s**.

$$q = q_m * \frac{b * p^{1/n}}{1 + b * p^{1/n}} \qquad (1)$$

where p is the pressure of the bulk gas at equilibrium with the adsorbed phase (kPa), q is the adsorbed amount per mass of adsorbent (mmol g^{-1}), q_m is the saturation capacities of site (mmol g^{-1}), b is the affinity coefficients of site (1/kPa), and n represent the deviations from an ideal homogeneous surface.

On the base of the equation parameters of pure gas adsorption, the IAST model was further used to investigate the separation of C_2H_2/CO_2, CO_2/CH_4, C_2H_2/CH_4 and C_2H_4/CH_4, the adsorption selectivity is defined by

$$s_{A/B} = \frac{x_A / y_A}{x_B / y_B} \qquad (2)$$

Where x_i and y_i are the mole fractions of component *i* (*i* = A and B) in the adsorbed and bulk phases, respectively. Note that in the Henry regime $S_{A/B}$ is identical to the ratio of the Henry constants of the two species.

Topology Analysis for SNNU-65s.

Prior to topological analysis, the structure has been simplified to its points of extension (carboxylate C atoms of the linker), the trigonal PTC ligand can be simplified as a 3-connected node having triangle geometry, and while the di-copper paddlewheel SBUs and μ_3-O trimer cluster are then reduced to a 4-connected node (plane quadrilateral geometry) and 6-connected node (trigonal-prismatic geometry), respectively. The **SNNU-65s** exhibits vertex 3-transitive (3,4,6)-connected *agw* net:

Point symbol for net: $\{6^3\}_6\{6^4.8^2\}_3\{6^6.8^3.10^6\}$

TD10 = 1054

Topological terms for each node:

(V1 for PTC ligand) Point symbol: $\{6^3\}$

Extended point symbol: [6.6.6(2)]

Coordination sequence: 3 11 18 47 53 117 108 209 179 331

(V2 for the di-copper paddlewheel) Point symbol: $\{6^4.8^2\}$

Extended point symbol: [6.6.6(2).6(2).8(2).8(2)]

Coordination sequence: 4 8 26 36 76 68 162 158 264 192

(V3 for μ_3-O trimer cluster) Point symbol: $\{6^6.8^3.10^6\}$

Extended point symbol: [6.6.6.6.6.6.8(2).8(2).8(2).10(4).10(4).10(4).10(4).10(4).10(4)]

Coordination sequence: 6 12 30 32 90 96 162 122 282 264

Transitivity: [3233]

Tilling: $[6^2.8^3] + [6^6] + [6^8.8^3]$

Topological type: *agw*

S2. Tables in Electronic Supplementary Information

Table S1. The Crystal data and structure refinements for **SNNU-65-Cu-Ga**.

Formula	$C_{90}H_{51}Cu_6Ga_3O_{46}$
Formula weight	2458.71
Temperature (K)	153(2)
Crystal system	hexagonal
Space group	*P*6(3*)/mmc*
a(Å)	18.5324(10)
b(Å)	18.5324(10)
c(Å)	40.250(4)
α (deg)	90.00
β (deg)	90.00
γ (deg)	120.00
Volume(Å^3)	11971.7(16)
Z	2
$d_{calcd.}$ (g·cm^{-3})	0.682
μ(mm^{-1})	0.893
F(000)	2452
Reflections collected/unique	283354 / 4576
R_{int}	0.0931
Data/restraints/parameters	4576 / 0 / 125
GOF on F^2	1.147
R_1[a], wR_2[b] [I > 2σ(I)]	0.0882, 0.1959
R_1[a], wR_2[b] (all data)	0.0992, 0.2029

[a] $R_1 = \Sigma||F_o|-|F_c||/\Sigma|F_o|$. [b] $wR_2= [\Sigma w(F_o^2 - F_c^2)^2/\Sigma w(F_o^2)^2]^{1/2}$.

Table S2. Selected bond lengths (Å) for **SNNU-65-Cu-Ga**.

Ga(1)-O(1)	2.073(10)	Cu(1)-O(4)	1.960(3)
Ga(1)-O(2)	1.9098(12)	Cu(1)-O(4)#1	1.960(3)
Ga(1)-O(3)	1.926(4)	Cu(1)-O(5)	2.123(5)
Ga(1)-O(3)#3	1.926(4)	Cu(1)-O(6)	1.946(3)
Ga(1)-O(3)#4	1.926(4)	Cu(1)-O(6)#1	1.946(3)
Ga(1)-O(3)#5	1.926(4)	Cu(1)-Cu(1)#2	2.6532(13)

Symmetry codes: #1: -x+y+1,y,z; #2: -x+1,-y,-z+1; #3: x,x-y,-z+3/2; #4: x,x-y,z; #5: x,y,-z+3/2.

Table S3. Summary of gas sorption properties for **SNNU-65** analogues.

SNNU-65s	**Cu-Sc**	**Cu-Fe**	**Cu-Ga**	**Cu-In**
S_A BET (m^2 g^{-1})	2089.2	2112.0	1918.0	1936.2
S_A Langmuir (m^2 g^{-1})	3274.5	3306.2	3013.4	3037.0
Pore volume (cm^3 g^{-1})	1.14	1.15	1.05	1.06
H_2 77 K, 1 atm (cm^3 g^{-1}/wt%)	268.7/2.4	267.9/2.4	236.0/2.1	237.7/2.1
CO_2 273 K, 1 atm (cm^3 g^{-1})	134.5	127.3	107.4	112.0
CO_2 298 K, 1 atm (cm^3 g^{-1})	70.4	64.9	58.7	56.1
Q_{st} (kJ/mol) for CO_2	22.2	21.8	20.5	24.9
CH_4 273 K, 1 atm (cm^3 g^{-1})	25.2	27.5	24.4	24.7
CH_4 298 K, 1 atm (cm^3 g^{-1})	16.6	15.3	13.6	13.8
Q_{st} (kJ/mol) for CH_4	11.6	16.6	15.2	15.8
C_2H_4 273 K, 1 atm (cm^3 g^{-1})	205.6	187.2	165.8	170.4
C_2H_4 298 K, 1 atm (cm^3 g^{-1})	122.5	112.9	98.8	105.1
Q_{st} (kJ/mol) for C_2H_4	61.4	23.5	31.1	24.8
C_2H_2 273 K, 1 atm (cm^3 g^{-1})	287.2	269.7	228.7	251.2
C_2H_2 298 K, 1 atm (cm^3 g^{-1})	178.9	162.3	141.6	153.3
Q_{st} (kJ/mol) for C_2H_2	44.9	28.2	31.7	23.4

Table S4. Contributions of open metal sites (OMSs) and pore space in acetylene uptakes for selected top-performing MOFs at room temperature and 1 atm for gravimetric capacity and comparison of equimolar C_2H_2/CO_2 and C_2H_2/CH_4 selective data under 1 atm by IAST.*

MOFs	**SBET (m^2 g^{-1})**	**OMS density (mmol g^{-1})**	**C_2H_2 uptake (cm^3 g^{-1})**			**IAST selectivity (50-50)**		**Ref.**
			By OMS	**By pore space**	**Sum**	**C_2H_2/ CO_2**	**C_2H_2/ CH_4**	
SNNU-65-Cu-Sc	2089.2	3.57	86	92.9	178.9	13.5	115.5	
SNNU-65-Cu-Fe	2112.0	3.52	85	77.3	162.3	6.7	37.3	
SNNU-65-Cu-Ga	1918.0	3.46	84	57.6	141.6	18.7	120.6	
SNNU-65-Cu-In	1936.2	3.26	79	74.3	153.3	7.0	69.5	
HKUST-1	1401	4.96	120	81	201.0	11.0	-	5
UTSA-50[a]	604	-	-	-	91.0	13.3	68.0	6
ZJU-40	2858	-	-	-	216.0	11.5	-	7
ZJU-195	1721.9	-	-	-	214.2	4.7	43.4	8
ZJU-199	987	-	-	-	128.0	4.0	27.3	9
UTSA-222	703	-	-	-	85.3	4.0	19.0	10

*The room temperature with range of being from 295 to 298 °C.

The open metal site (OMS) density was calculated based on the crystal information file.

[a] The selectivity predicted by Henry's law.

S3. Figures in Electronic Supplementary Information

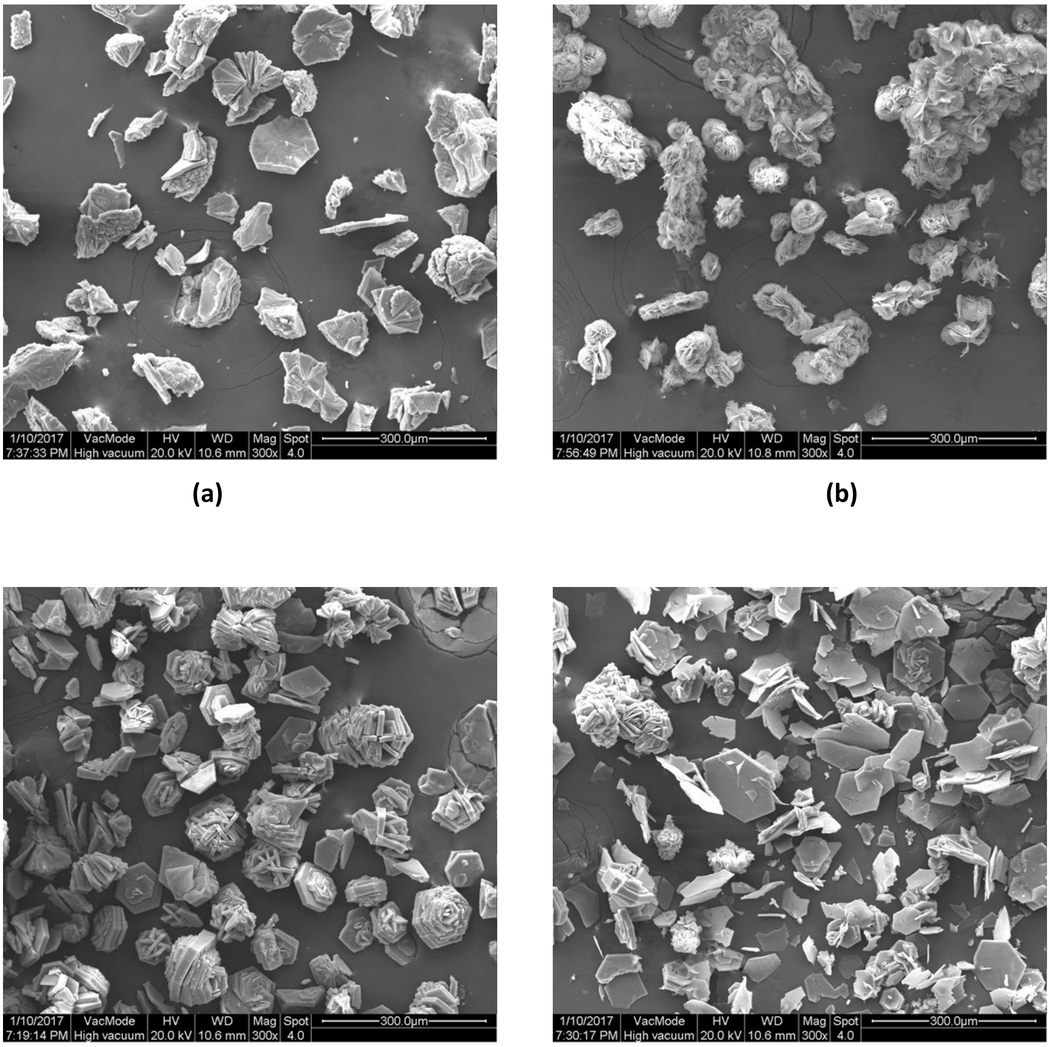

(a) **(b)**

(c) **(d)**

Figure S1. Scanning electron microscope photographs of **SNNU-65s**: (a) **-Cu**-**Sc**; (b) **-Cu**-**Fe**; (c) **-Cu**-**Ga** and (d) **-Cu**-**In**.

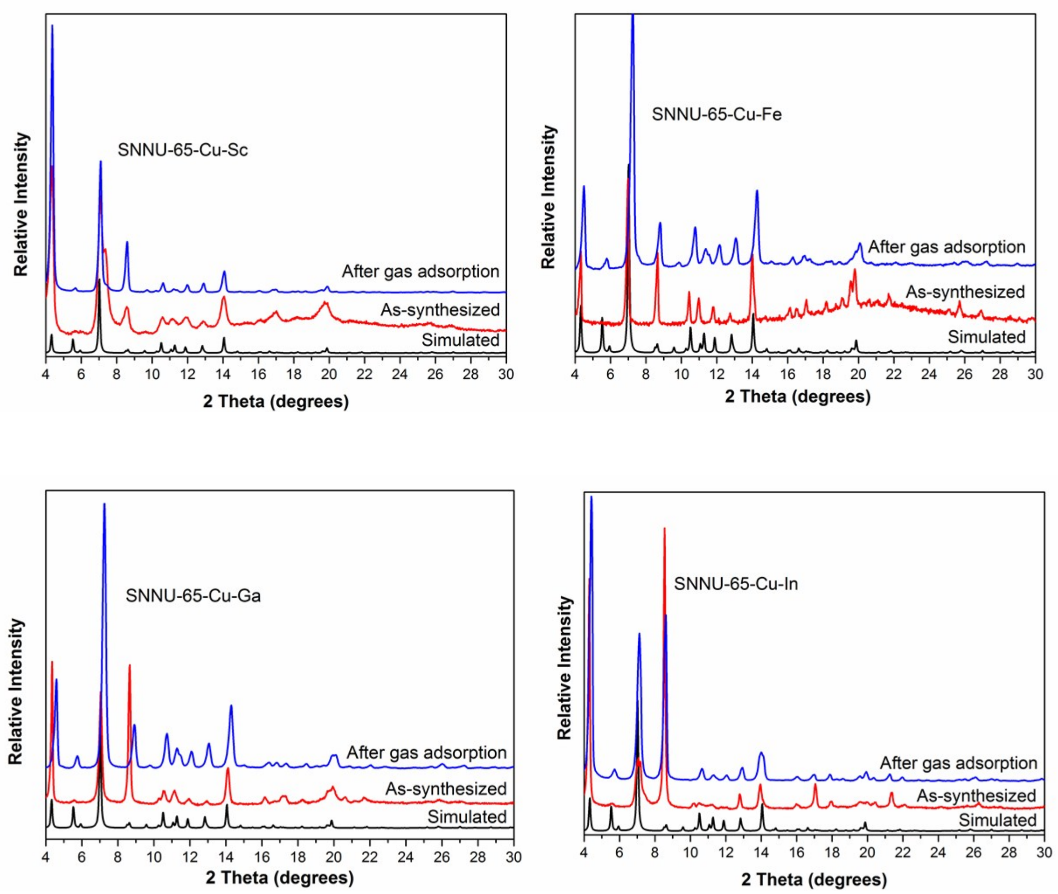

Figure S2. PXRD patterns for **SNNU-65s**.

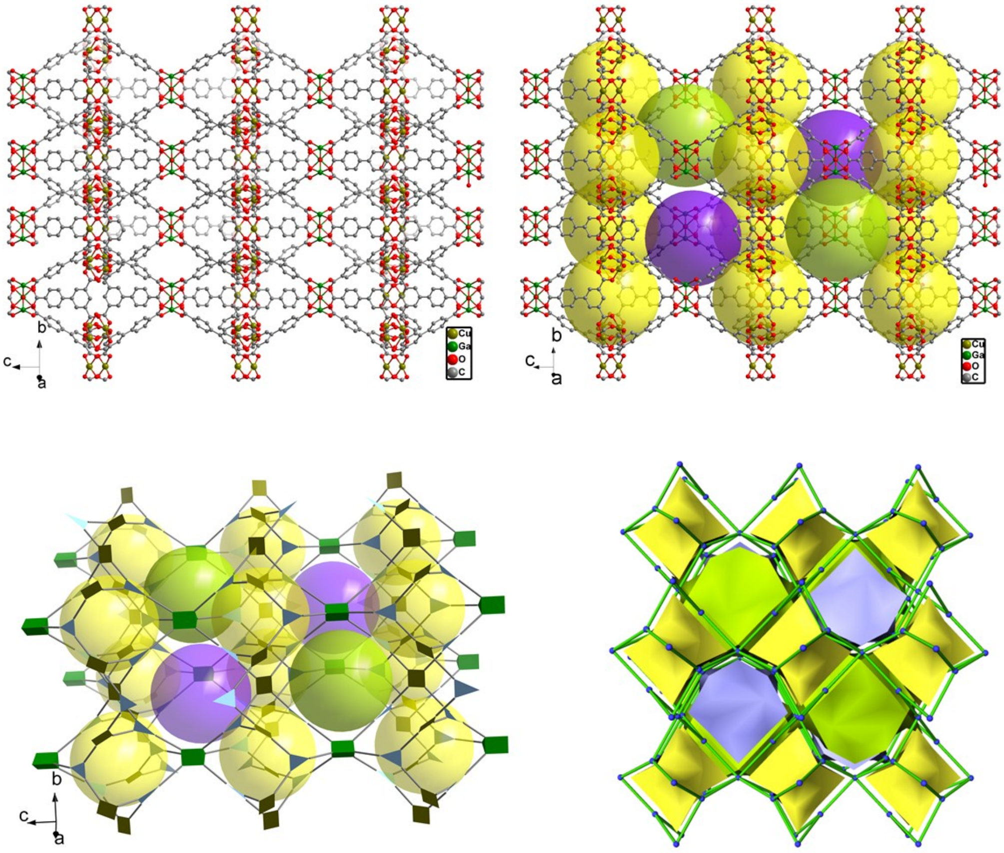

Figure S3. Structure of porous frameworks and tiling representation of **SNNU-65s** (All the hydrogen atoms and the terminal water molecules are omitted for clarity.)

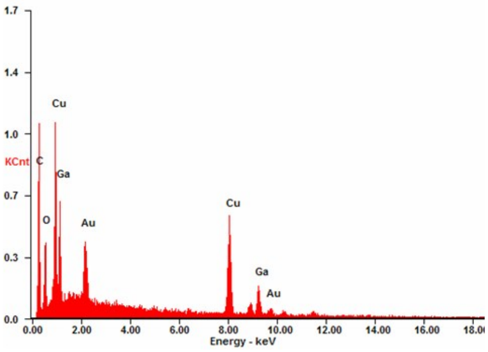

Element	*Wt %*	*At %*
C K	47.91	75.51
O K	10.57	12.51
CuK	26.68	07.95
GaK	14.84	04.03

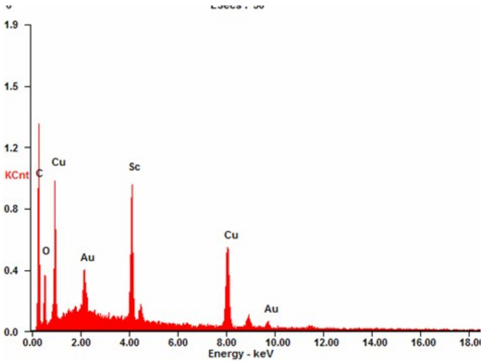

Element	*Wt %*	*At %*
C K	47.23	73.02
O K	11.83	13.73
ScK	10.61	04.38
CuK	30.32	08.86

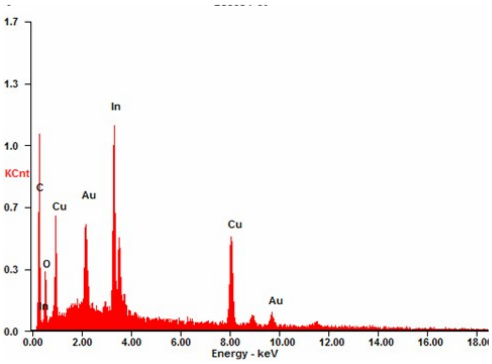

Element	*Wt %*	*At %*
C K	36.20	70.68
O K	09.16	13.43
InL	25.89	05.29
CuK	28.75	10.61

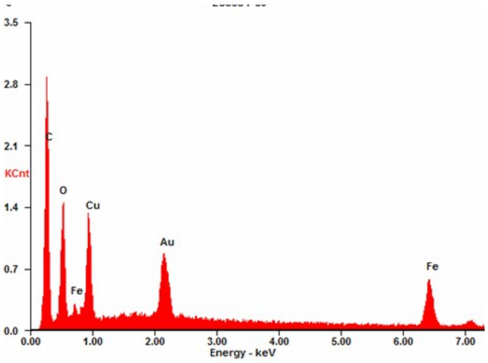

Element	*Wt %*	*At %*
C K	52.75	71.92
O K	20.40	20.88
FeK	08.00	02.35
CuK	18.86	04.86

Figure S4. Energy dispersive spectroscopy (EDS) of **SNNU-65s**.

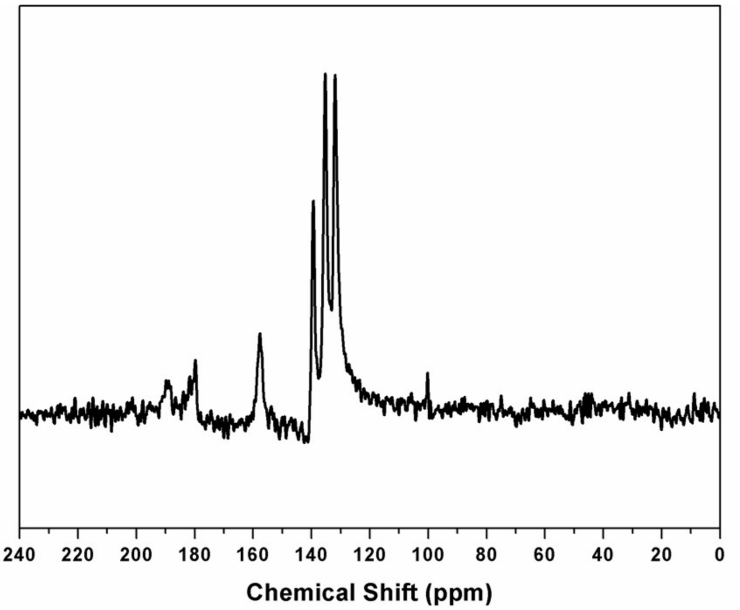

Figure S5. The solid state ^{13}C crosspolarization magicangle spinning (CP/MAS) NMR spectroscopy for the activated **SNNU-65-Cu-Ga s**ample, which indicated the absence of DMA$^+$ counterions.

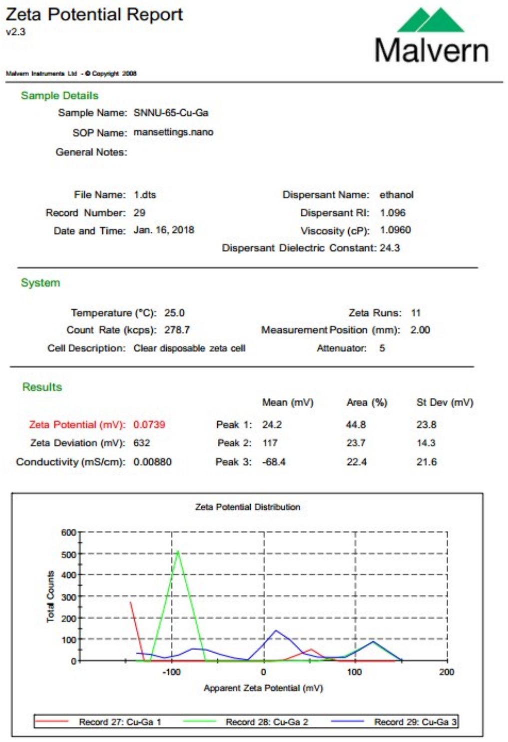

Zeta Potential Report
v2.3

Malvern

Malvern Instruments Ltd - © Copyright 2008

Sample Details

Sample Name: SNNU-65-Cu-Ga
SOP Name: mansettings.nano
General Notes:

File Name: 1.dts
Record Number: 29
Date and Time: Jan. 16, 2018
Dispersant Name: ethanol
Dispersant RI: 1.096
Viscosity (cP): 1.0960
Dispersant Dielectric Constant: 24.3

System

Temperature (°C): 25.0
Count Rate (kcps): 278.7
Cell Description: Clear disposable zeta cell
Zeta Runs: 11
Measurement Position (mm): 2.00
Attenuator: 5

Results

Zeta Potential (mV): 0.0739
Zeta Deviation (mV): 632
Conductivity (mS/cm): 0.00880

	Mean (mV)	Area (%)	St Dev (mV)
Peak 1:	24.2	44.8	23.8
Peak 2:	117	23.7	14.3
Peak 3:	-68.4	22.4	21.6

Figure S6. The Zeta potential result for **SNNU-65-Cu-Ga.**

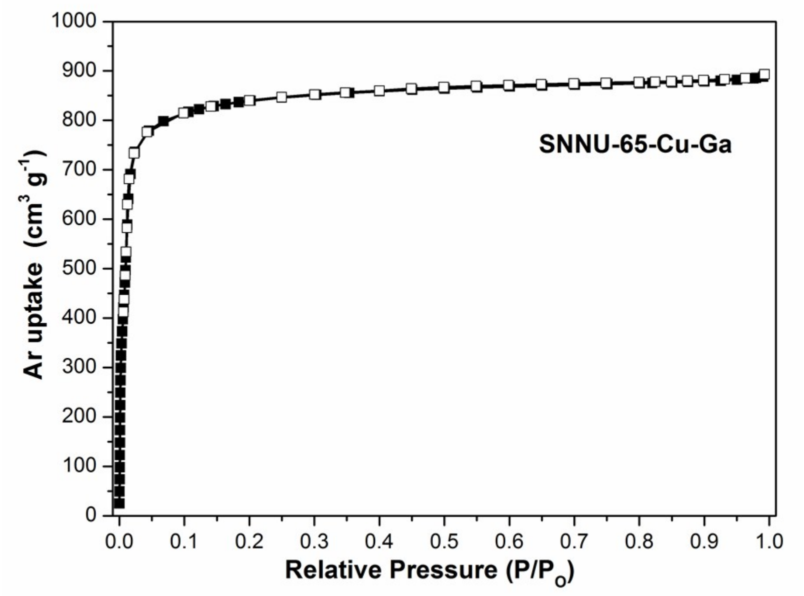

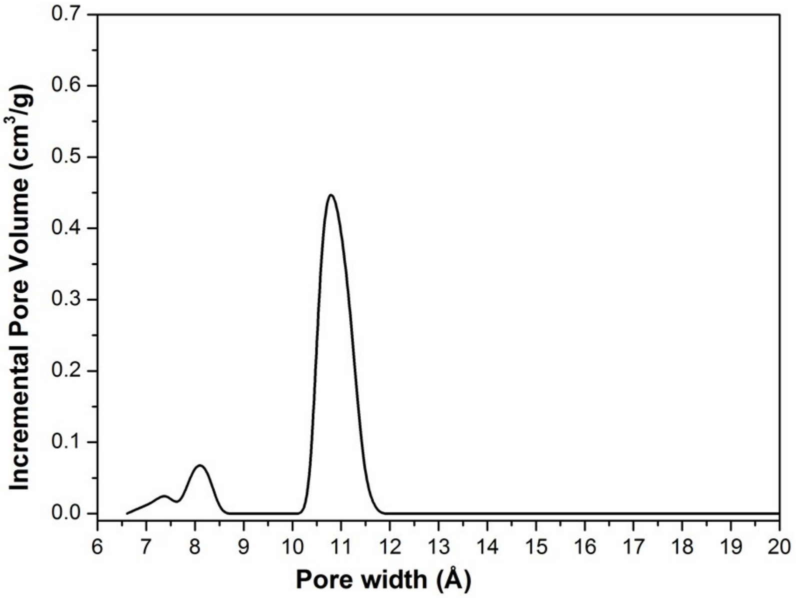

Figure S7. Ar adsorption and desorption isotherms of **SNNU-65-Cu-Ga** at 87 K (top) and the pore size distribution determined by analyzing the Ar isotherm using non-local density functional theory (NLDFT) (bottom).

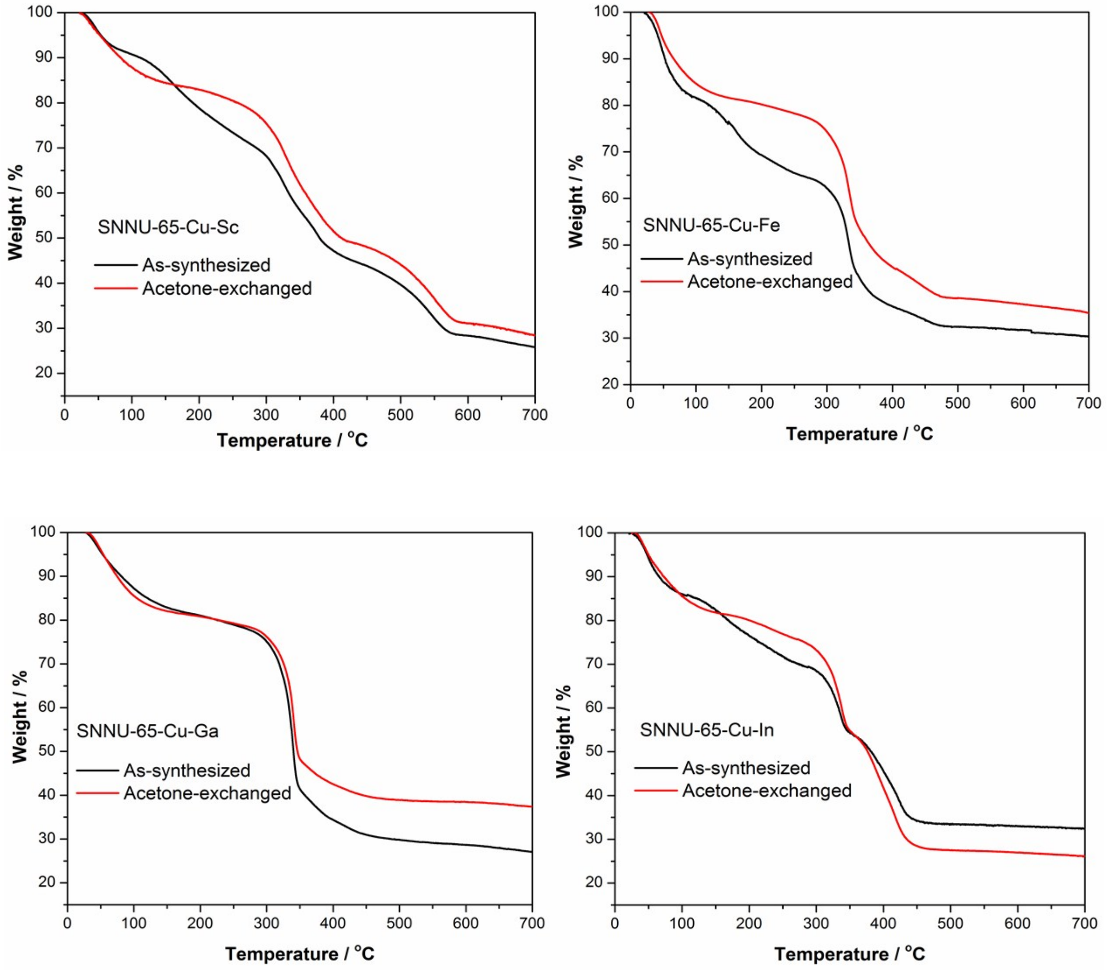

Figure S8. TGA curves of as-synthesized (black) and acetone-exchanged **SNNU-65s** (red).

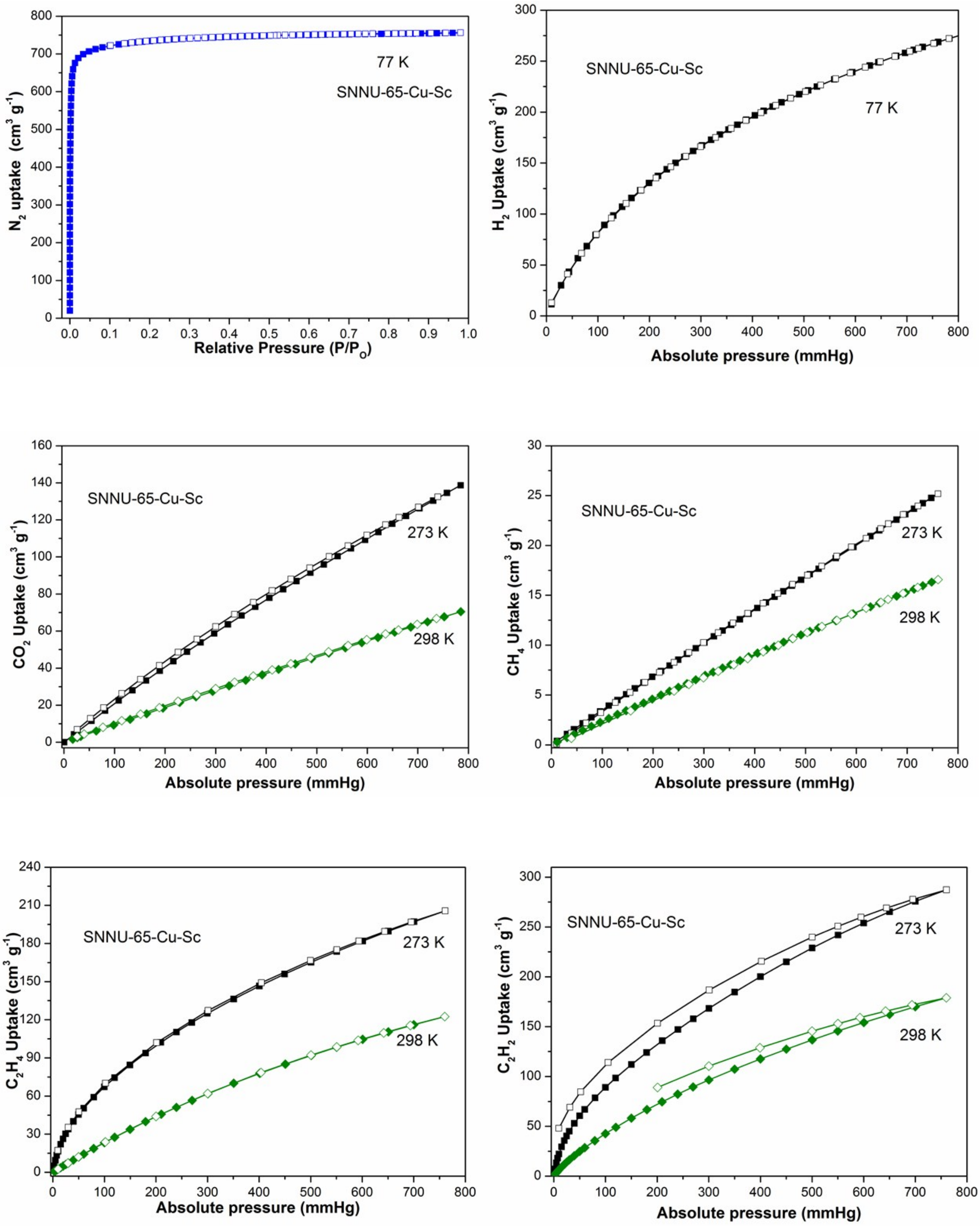

Figure S9. N_2, H_2, CO_2, CH_4, C_2H_4 and C_2H_2 adsorption and desorption isotherms of **SNNU-65-Cu-Sc**. Solid and open symbols indicate adsorption and desorption isotherms, respectively.

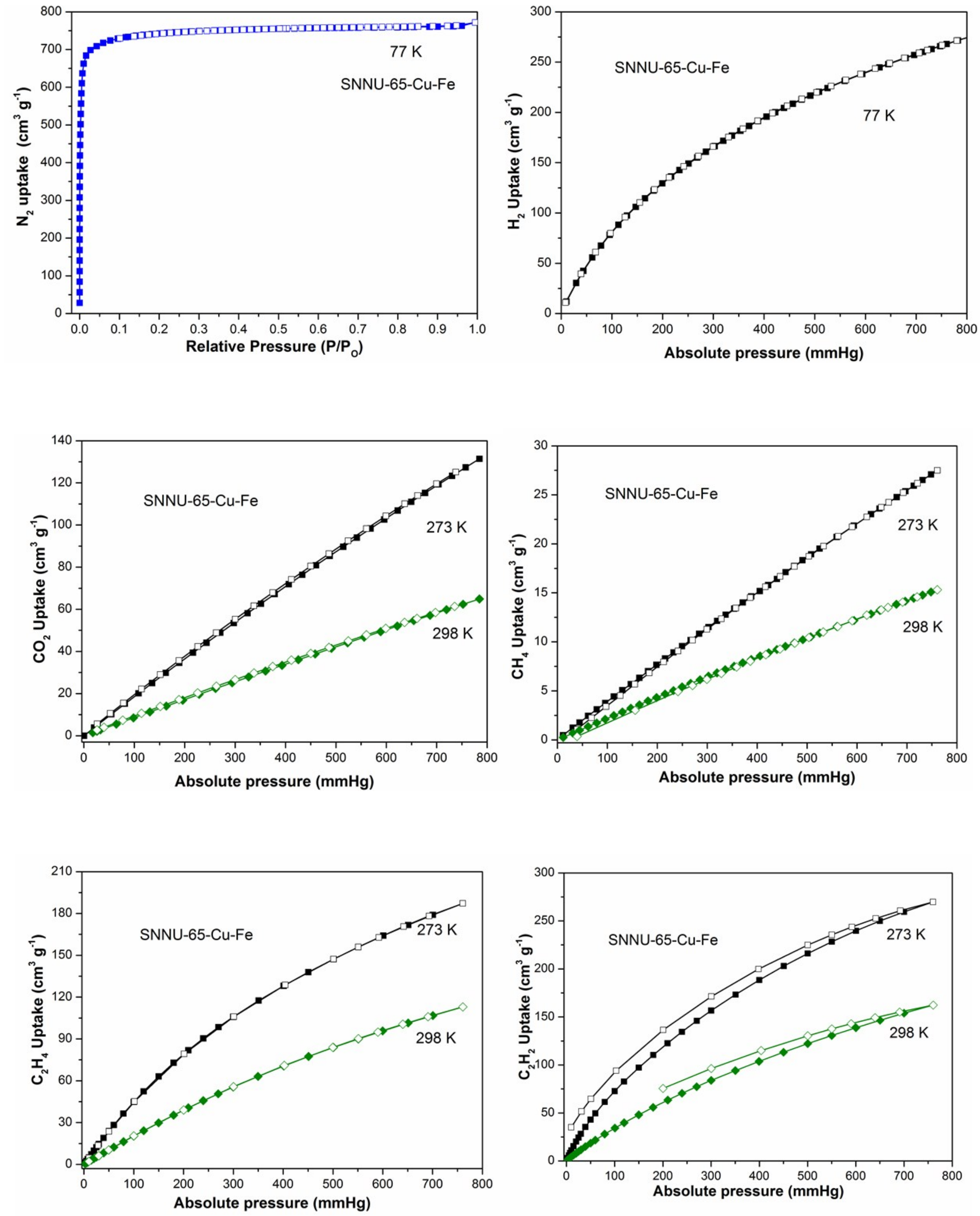

Figure S10. N_2, H_2, CO_2, CH_4, C_2H_4 and C_2H_2 adsorption and desorption isotherms of **SNNU-65-Cu-Fe**. Solid and open symbols indicate adsorption and desorption isotherms, respectively.

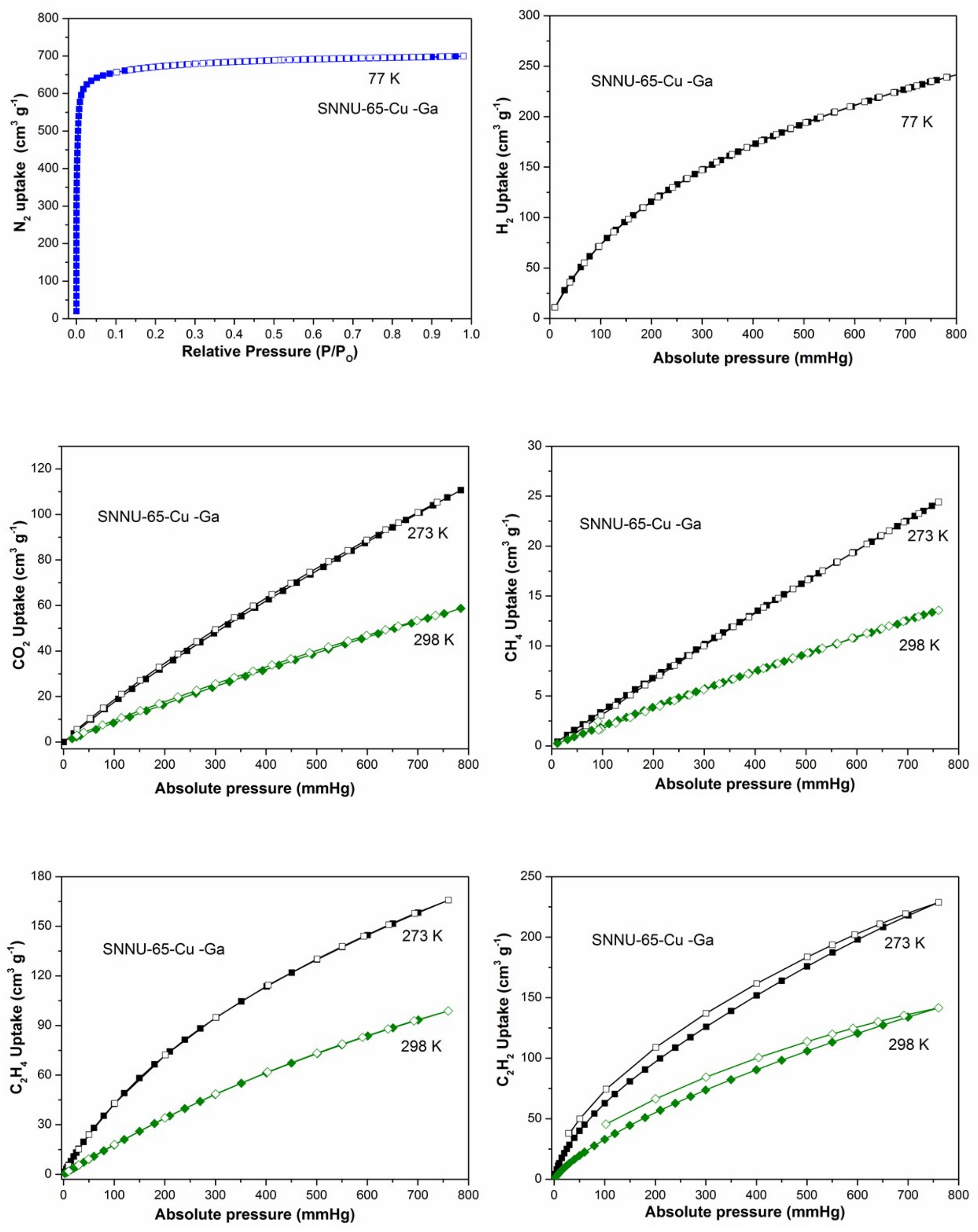

Figure S11. N_2, H_2, CO_2, CH_4, C_2H_4 and C_2H_2 adsorption and desorption isotherms of **SNNU-65-Cu-Ga**. Solid and open symbols indicate adsorption and desorption isotherms, respectively.

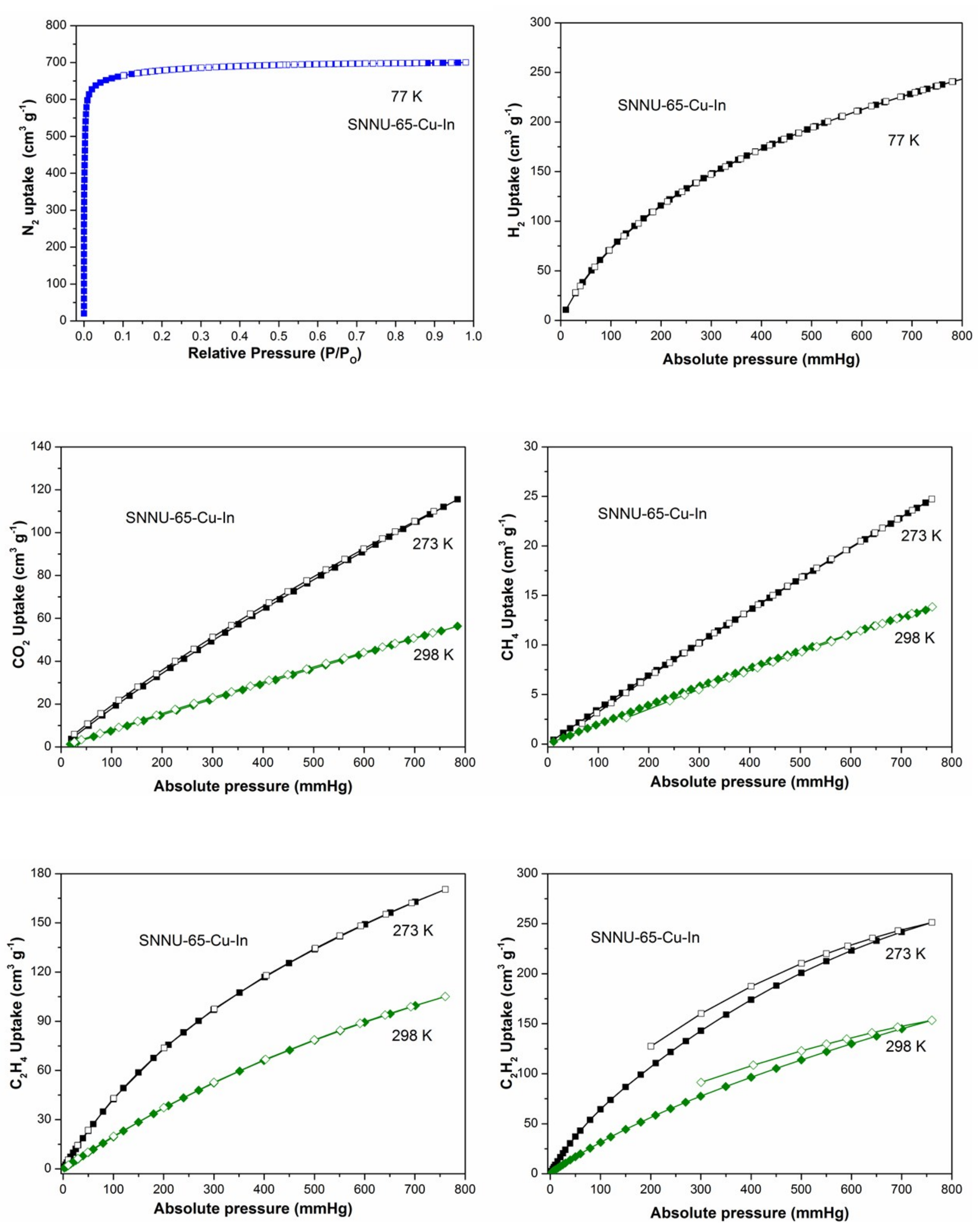

Figure S12. N_2, H_2, CO_2, CH_4, C_2H_4 and C_2H_2 adsorption and desorption isotherms of **SNNU-65-Cu-In**. Solid and open symbols indicate adsorption and desorption isotherms, respectively.

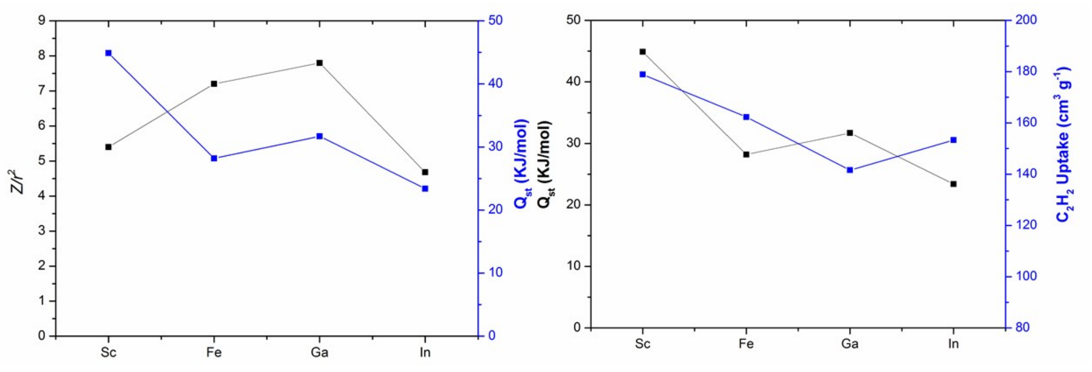

(a) **(b)**

Figure S13. (a) Correlation between isosteric heat at zero loading of C_2H_2 (Q_{st}) and charge-to-radius ratio (z/r^2) of M^{3+} ions. (b) Correlation between C_2H_2 (Q_{st}) and C_2H_2 uptakes for **SNNU-65s** at 1 atm and 298 K.

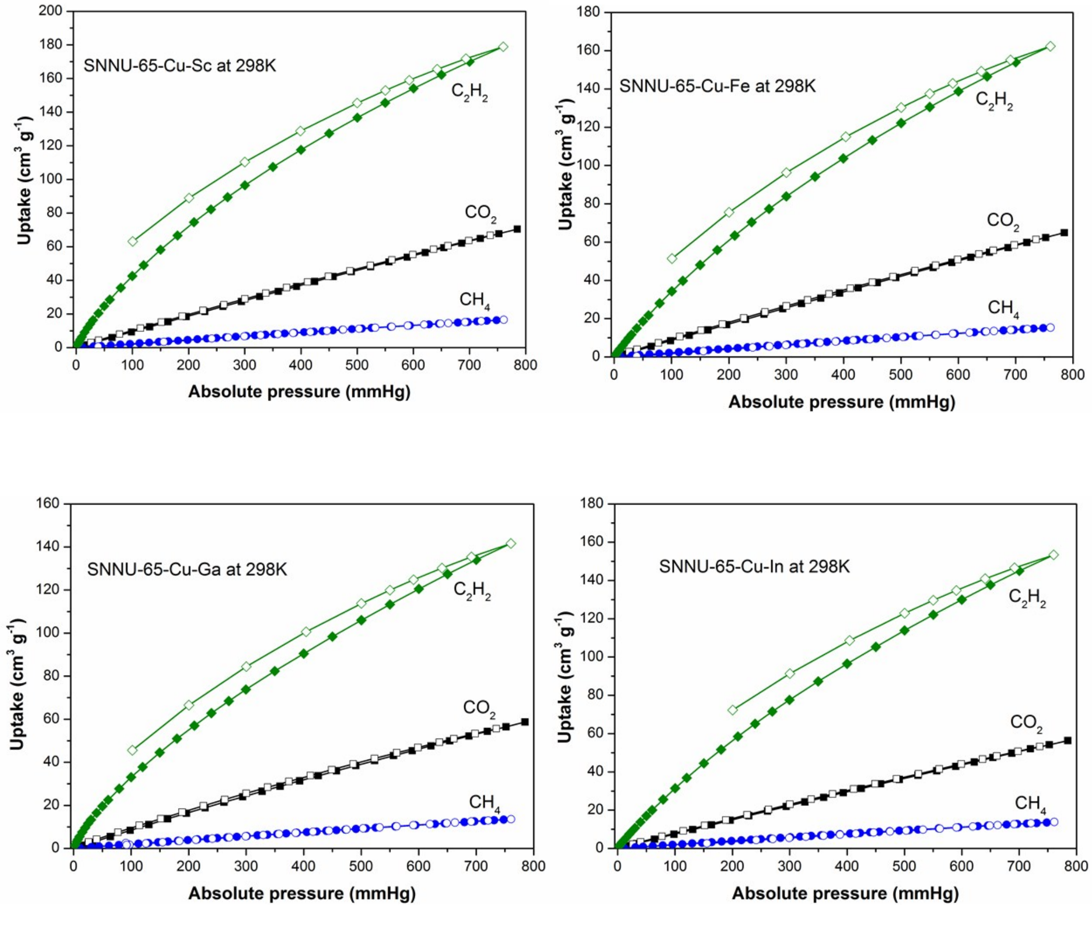

Figure S14. Comparison of C_2H_2, CO_2 and CH_4 adsorption isotherms for **SNNU-65s**.

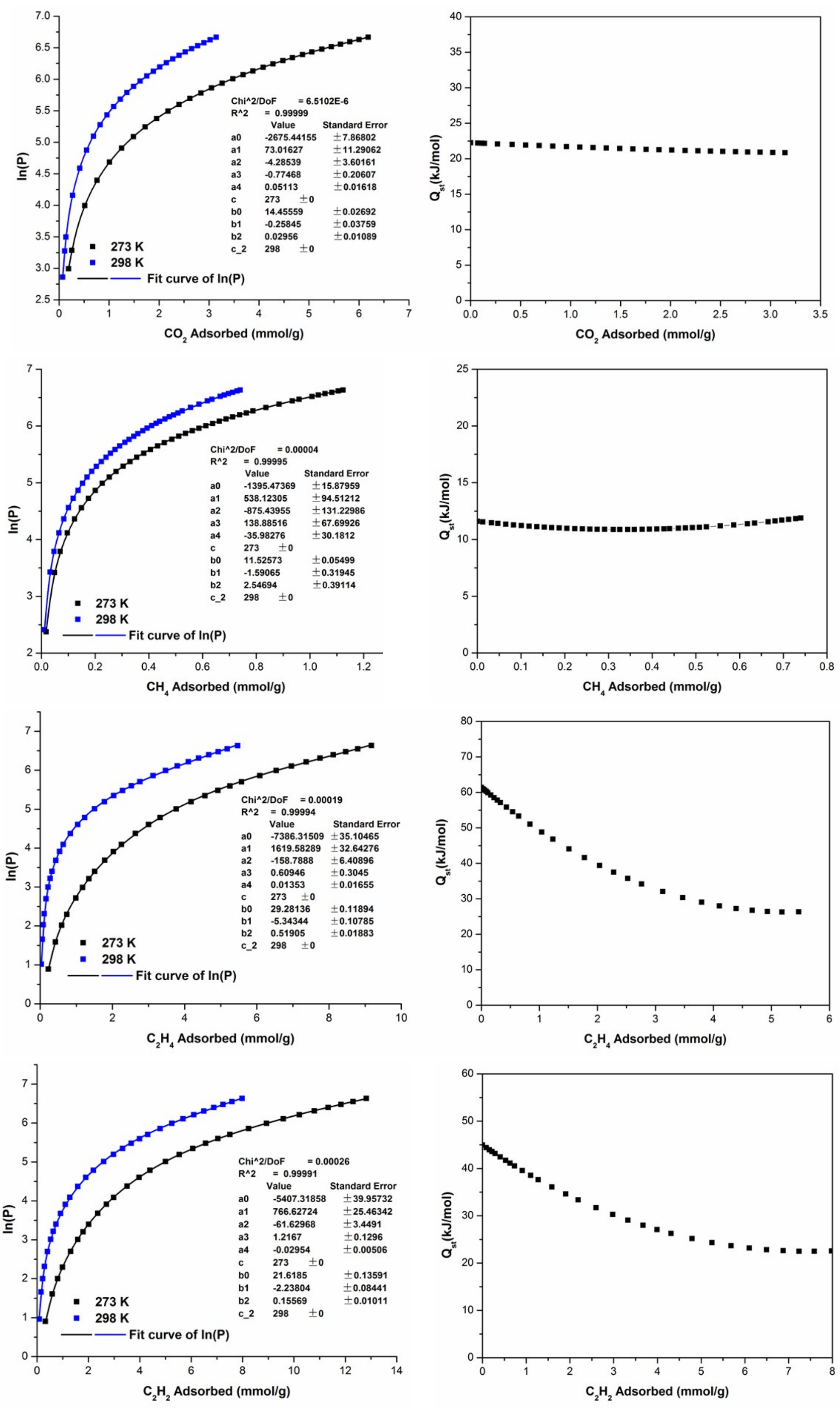

Chi^2/DoF = 6.5102E-6
R^2 = 0.99999

	Value	Standard Error
a0	-2675.44155	±7.86802
a1	73.01627	±11.29062
a2	-4.28539	±3.60161
a3	-0.77468	±0.20607
a4	0.05113	±0.01618
c	273 ±0	
b0	14.45559	±0.02692
b1	-0.25845	±0.03759
b2	0.02956	±0.01089
c_2	298 ±0	

Chi^2/DoF = 0.00004
R^2 = 0.99995

	Value	Standard Error
a0	-1395.47369	±15.87959
a1	538.12305	±94.51212
a2	-875.43955	±131.22986
a3	138.88516	±67.69926
a4	-35.98276	±30.1812
c	273 ±0	
b0	11.52573	±0.05499
b1	-1.59065	±0.31945
b2	2.54694	±0.39114
c_2	298 ±0	

Chi^2/DoF = 0.00019
R^2 = 0.99994

	Value	Standard Error
a0	-7386.31509	±35.10465
a1	1619.58289	±32.64276
a2	-158.7888	±6.40896
a3	0.60946	±0.3045
a4	0.01353	±0.01655
c	273 ±0	
b0	29.28136	±0.11894
b1	-5.34344	±0.10785
b2	0.51905	±0.01883
c_2	298 ±0	

Chi^2/DoF = 0.00026
R^2 = 0.99991

	Value	Standard Error
a0	-5407.31858	±39.95732
a1	766.62724	±25.46342
a2	-61.62968	±3.4491
a3	1.2167	±0.1296
a4	-0.02954	±0.00506
c	273 ±0	
b0	21.6185	±0.13591
b1	-2.23804	±0.08441
b2	0.15569	±0.01011
c_2	298 ±0	

Figure S15. Fitted gas adsorption isotherms of **SNNU-65-Cu-Sc** measured at 273 and 298 K, and their corresponding isosteric heats of adsorption (Q_{st}).

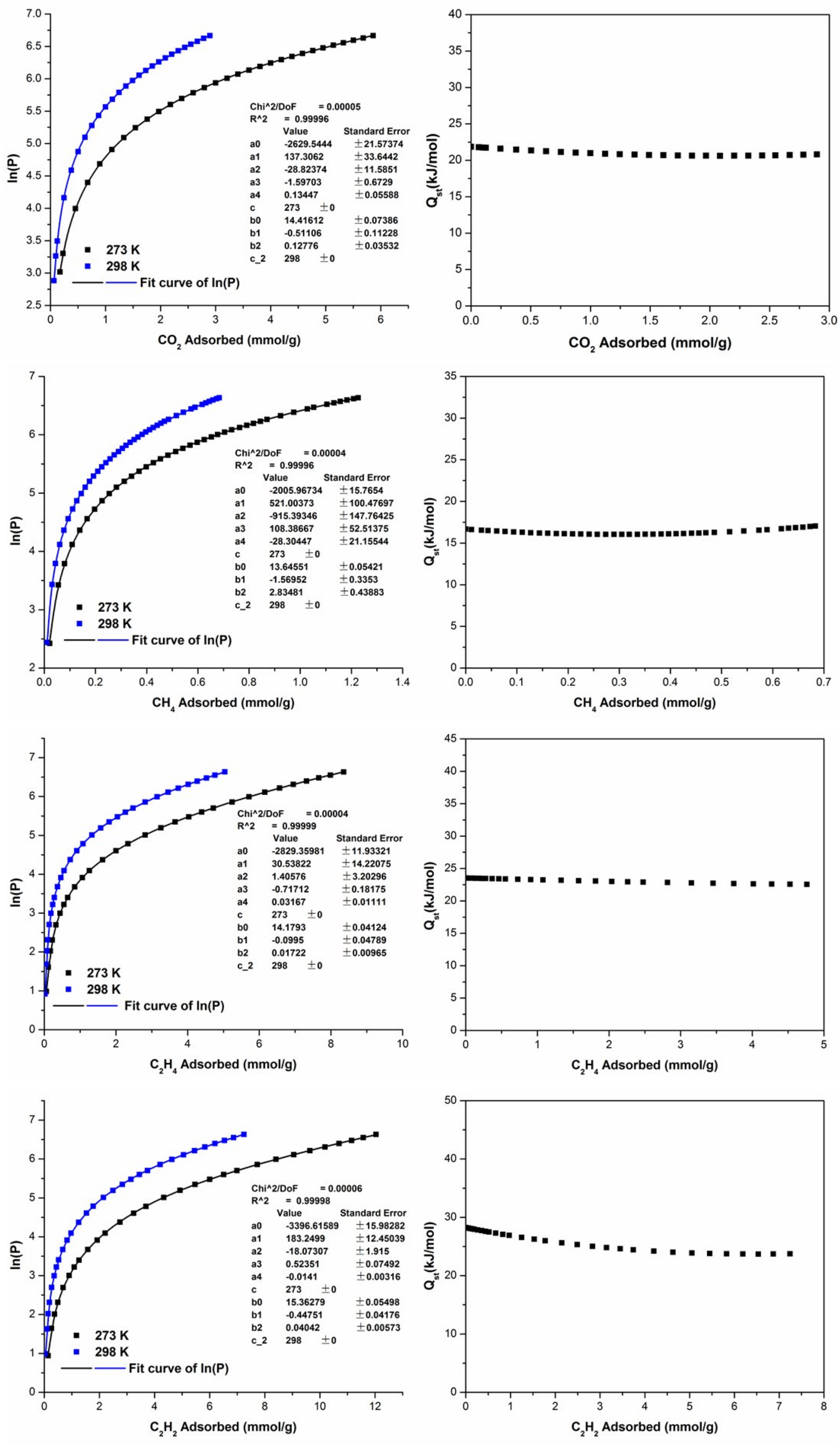

Chi^2/DoF = 0.00005
R^2 = 0.99996

	Value	Standard Error
a0	-2629.5444	±21.57374
a1	137.3062	±33.6442
a2	-28.82374	±11.5851
a3	-1.59703	±0.6729
a4	0.13447	±0.05588
c	273 ±0	
b0	14.41612	±0.07386
b1	-0.51106	±0.11228
b2	0.12776	±0.03532
c_2	298 ±0	

Chi^2/DoF = 0.00004
R^2 = 0.99996

	Value	Standard Error
a0	-2005.96734	±15.7654
a1	521.00373	±100.47697
a2	-915.39346	±147.76425
a3	108.38667	±52.51375
a4	-28.30447	±21.15544
c	273 ±0	
b0	13.64551	±0.05421
b1	-1.56952	±0.3353
b2	2.83481	±0.43883
c_2	298 ±0	

Chi^2/DoF = 0.00004
R^2 = 0.99999

	Value	Standard Error
a0	-2829.35981	±11.93321
a1	30.53822	±14.22075
a2	1.40576	±3.20296
a3	-0.71712	±0.18175
a4	0.03167	±0.01111
c	273 ±0	
b0	14.1793	±0.04124
b1	-0.0995	±0.04789
b2	0.01722	±0.00965
c_2	298 ±0	

Chi^2/DoF = 0.00006
R^2 = 0.99998

	Value	Standard Error
a0	-3396.61589	±15.98282
a1	183.2499	±12.45039
a2	-18.07307	±1.915
a3	0.52351	±0.07492
a4	-0.0141	±0.00316
c	273 ±0	
b0	15.36279	±0.05498
b1	-0.44751	±0.04176
b2	0.04042	±0.00573
c_2	298 ±0	

Figure S16. Fitted gas adsorption isotherms of **SNNU-65-Cu-Fe** measured at 273 K and 298 K, and their corresponding isosteric heats of adsorption (*Q*$_{st}$).

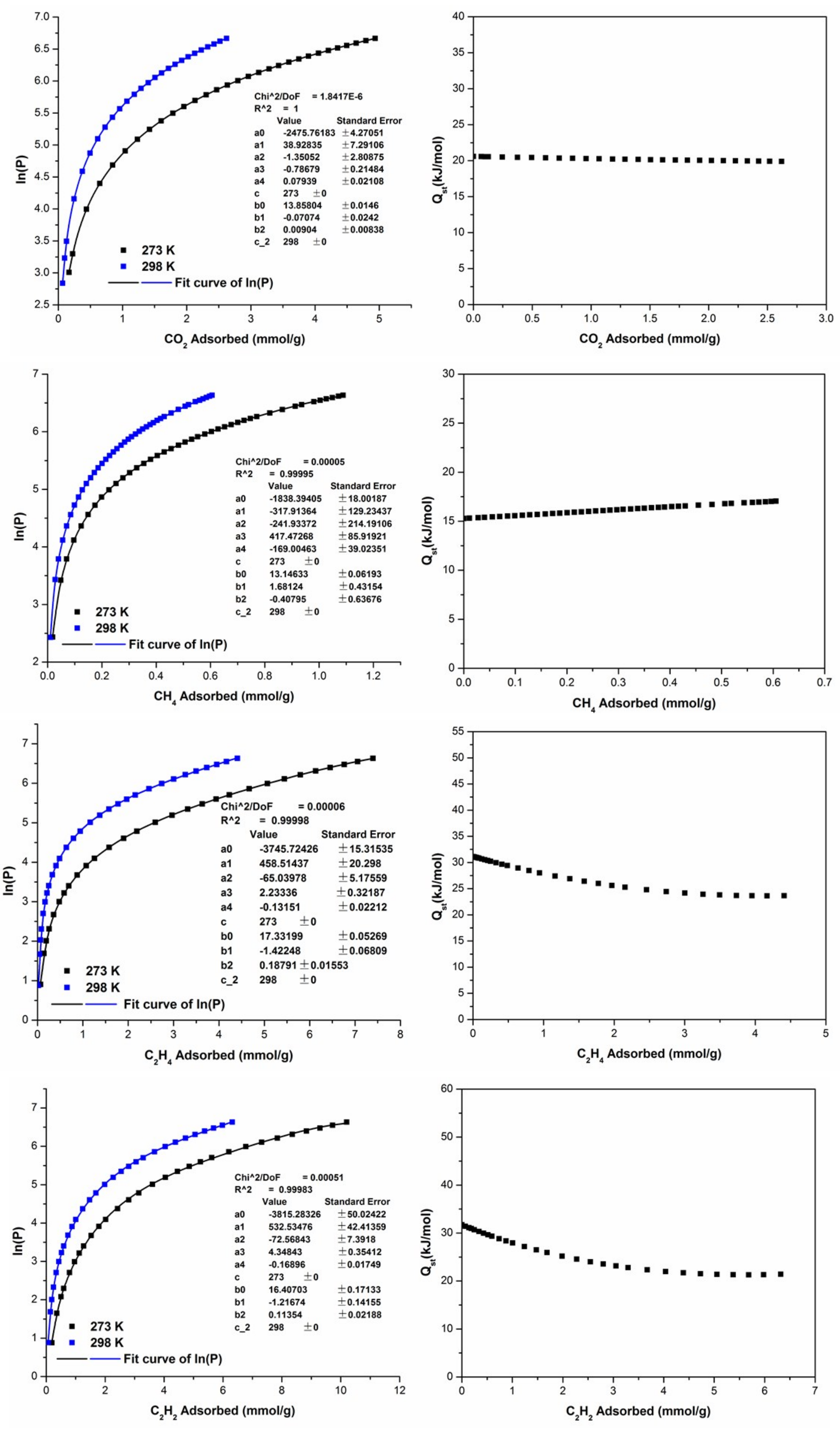

Figure S17. Fitted gas adsorption isotherms of **SNNU-65-Cu-Ga** measured at 273 K and 298 K, and their corresponding isosteric heats of adsorption (Q_{st}).

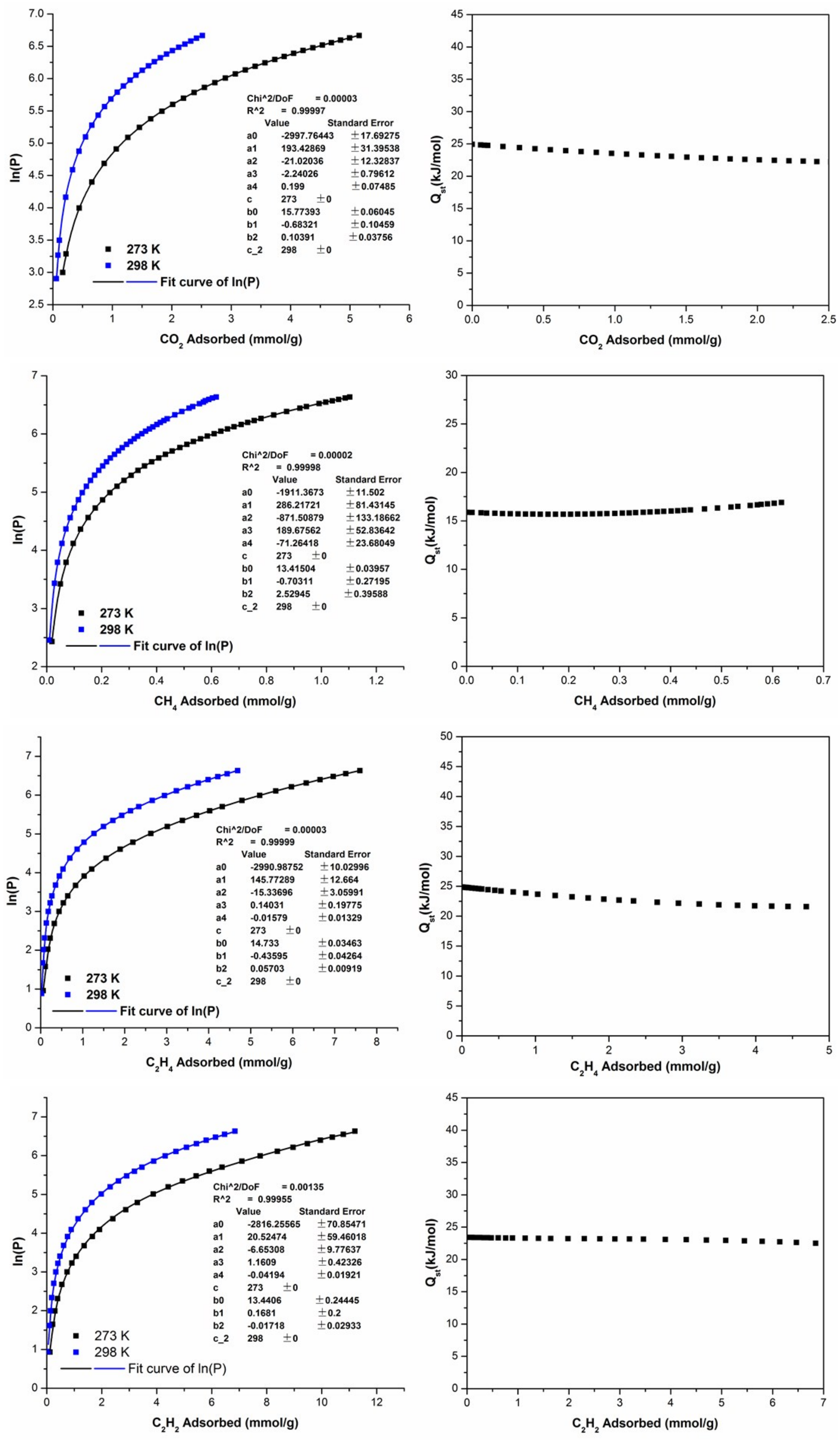

Figure S18. Fitted gas adsorption isotherms of **SNNU-65-Cu-In** measured at 273 K and 298 K, and their corresponding isosteric heats of adsorption (Q_{st}).

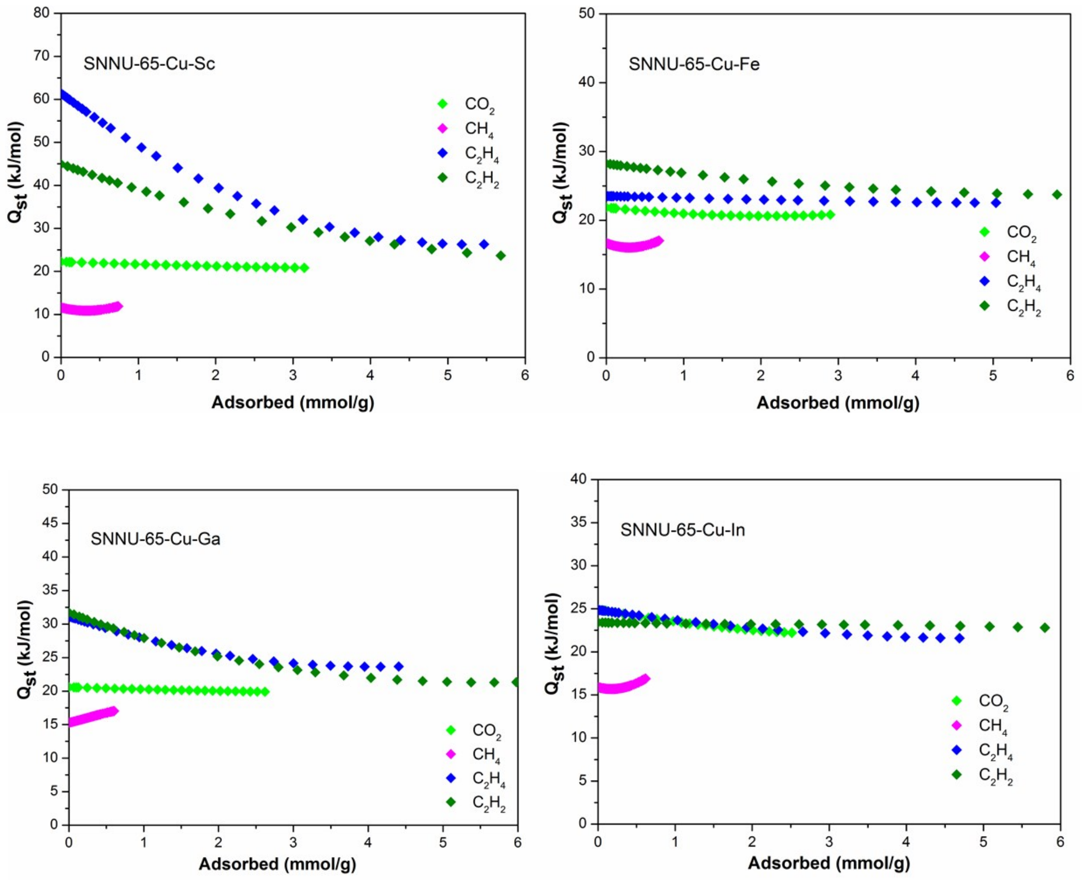

Figure S19. Comparison of the isosteric heats of adsorption (Q_{st}) of **SNNU-65s**.

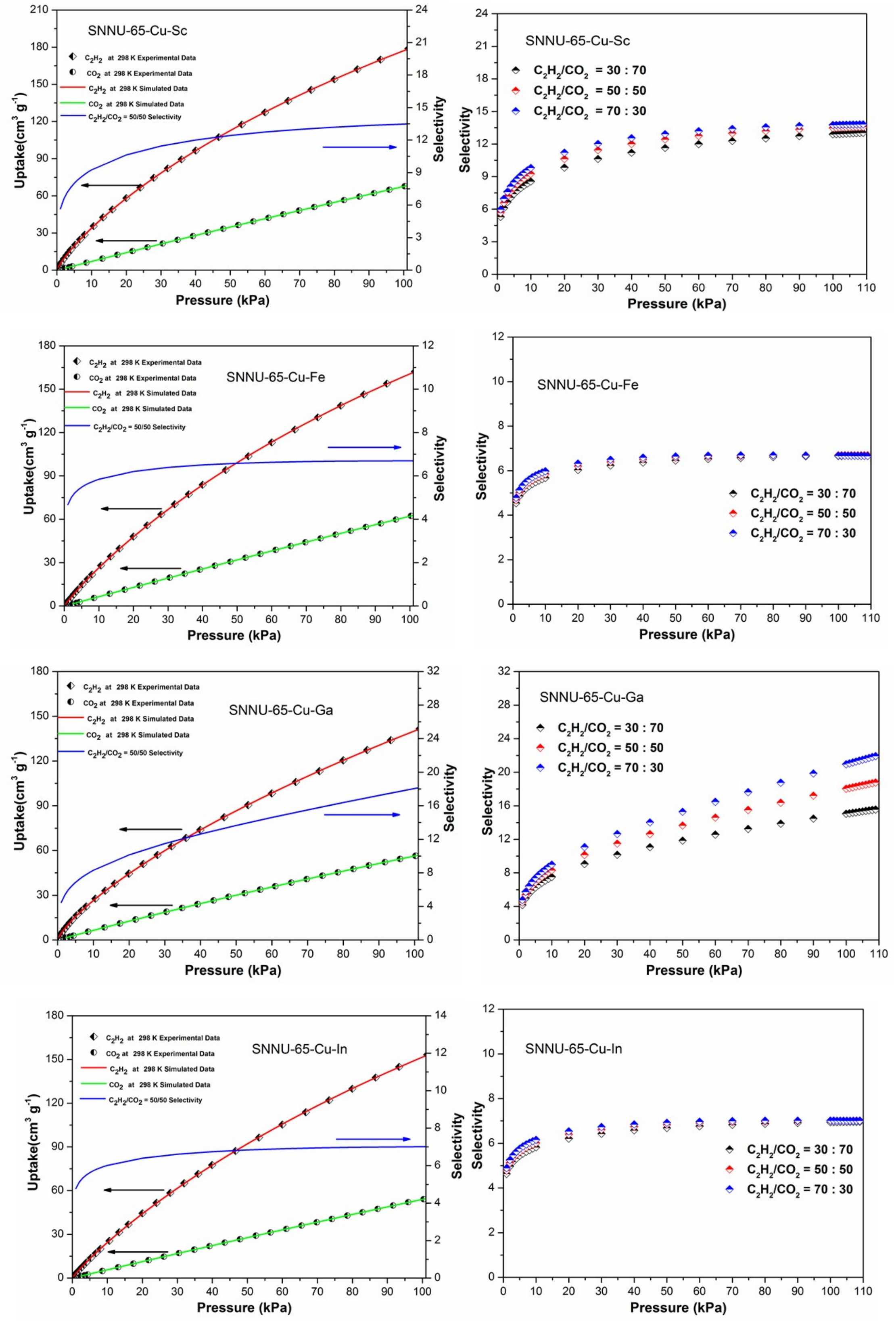

Figure S20. Comparison of experimental and simulated isotherms and adsorption selectivity for C_2H_2/CO_2 binary-mixture predicted by IAST of **SNNU-65s** at 298 K.

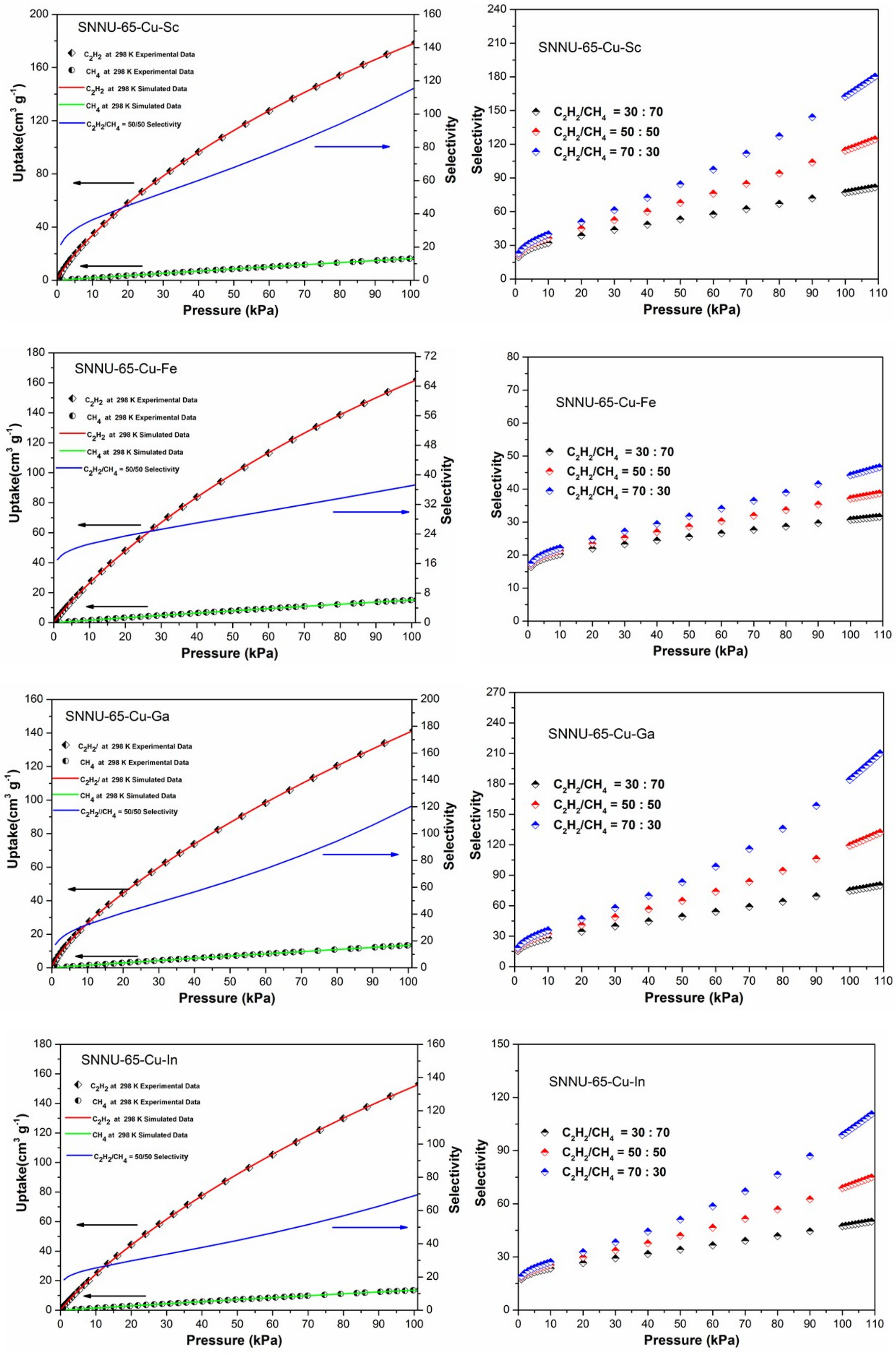

Figure S21. Comparison of experimental and simulated isotherms and adsorption selectivity for C_2H_2/CH_4 binary-mixture predicted by IAST of **SNNU-65s** at 298 K.

References

1 (a) G. M. Sheldrick, *SHELXS 97: Program for the Solution of Crystal Structure*; University of Göttingen: Göttingen, Germany, 1997; (b) G. M. Sheldrick, *SHELXS 97: Program for the Crystal Structure Refinement*; University of Göttingen: Göttingen, Germany, 1997**;** (c) G. M. Sheldrick, *SADABS: Siemens Area correction Absorption Program*; University of Göttingen: Göttingen, Germany, 1994.

2 A. L. Spek, *J. Appl. Crystallogr*., 2003, **36**, 7.

3 J. L. C. Rowsell and O. M. Yaghi, *J. Am. Chem. Soc.*, 2006, **128**, 1304.

4 (a) A. L. Myers and J. M. Prausnitz, *AIChE J.*, 1965, **11**, 121; (b) Y.-S. Bae, K. L. Mulfort, H. Frost, P. Ryan, S. Punnathanam, L. J. Broadbelt, J. T. Hupp and R. Q. Snurr, *Langmuir*, 2008, **24**, 8592.

5 S. Xiang, W. Zhou, J. M. Gallegos, Y. Liu and B. Chen, *J. Am. Chem. Soc.*, 2009, **131**, 12415.

6 H. Xu, Y. He, Z. Zhang, S. Xiang, J. Cai, Y. Cui, Y. Yang, G. Qian and B. Chen, *J. Mater. Chem. A*, 2013, **1**, 77.

7 H.-M. Wen, H. Wang, B. Li, Y. Cui, H. Wang, G. Qian and B. Chen, *Inorg. Chem.*, 2016, **55**, 7214.

8 L. Zhang, K. Jiang, Y. Li, D. Zhao, Y. Yang, Y. Cui, B. Chen and G. Qian, *Cryst. Growth Des.*, 2017, **17**, 2319.

9 L. Zhang, C. Zou, M. Zhao, K. Jiang, R. Lin, Y. He, C.-D. Wu, Y. Cui, B. Chen and G. Qian, *Cryst. Growth Des.*, 2016, **16**, 7194.

10 J. Ma, J. Guo, H. Wang, B. Li, T.Yang and B. Chen, *Inorg. Chem.*, 2017, **56**, 7145.